Singlet Oxygen Involved Luminol Chemiluminescence Catalyzed by Graphene Oxide

ARTICLE *in* THE JOURNAL OF PHYSICAL CHEMISTRY C · SEPTEMBER 2012

Impact Factor: 4.77 · DOI: 10.1021/jp306061u

6 AUTHORS, INCLUDING:

Yi Wang
Chongqing Normal University
37 PUBLICATIONS **931** CITATIONS
SEE PROFILE

Cheng Zhi Huang
xx
266 PUBLICATIONS **5,219** CITATIONS
SEE PROFILE

THE JOURNAL OF PHYSICAL CHEMISTRY C

Article

pubs.acs.org/JPCC

Singlet Oxygen Involved Luminol Chemiluminescence Catalyzed by Graphene Oxide

Dong Mei Wang,[†] Yan Zhang,[†] Lin Ling Zheng,[†] Xiao Xi Yang,[†] Yi Wang,[†] and Cheng Zhi Huang*[,†,‡]

[†]Education Ministry Key Laboratory on Luminescence and Real-Time Analysis, College of Chemistry and Chemical Engineering, and [‡]College of Pharmaceutical Sciences, Southwest University, 400715 Chongqing, PR China

Supporting Information

ABSTRACT: Singlet oxygen ($^1O_2$) in the chemiluminescence (CL) of luminol has been rarely involved. In this work, graphene oxide (GO) was prepared and at first found to enhance the CL of luminol-H_2O_2 system in a weakly alkaline medium mainly through the intermediate of $^1O_2$, which was greatly different from the traditional catalyst in such CL system that occurred in a strongly basic medium through the intermediates such as superoxide anion radical ($O_2^{\bullet-}$) and hydroxyl radical (OH•). With the aid of CL spectral, UV−visible absorption spectral, and electron spin resonance (ESR) spectral measurements and investigations on the effects of various free radical scavengers on the GO-enhanced luminol CL, we identified the acceleration role of GO played in the electron-transfer processes and efficient catalysis on the decomposition of H_2O_2, generating a high yield of $^1O_2$ on the surface of GO. The resulted $^1O_2$ then reacted with luminol, producing an endoperoxide, which decomposed to the excited-state 3-aminophthalate anions (3-APA*), giving rise to light emission with the maximum wavelength at 440 nm. As a result, this $^1O_2$-induced luminol CL, owing to the catalysis by GO, could have six-fold enhancement compared with that in the absence of GO. These investigations could be further extended to the use of GO as an amplified label for the CL determinations of H_2O_2 and glucose. The significant features of this GO-catalyzed luminol CL may open up new opportunities for its potential applications in a wide range of fields.

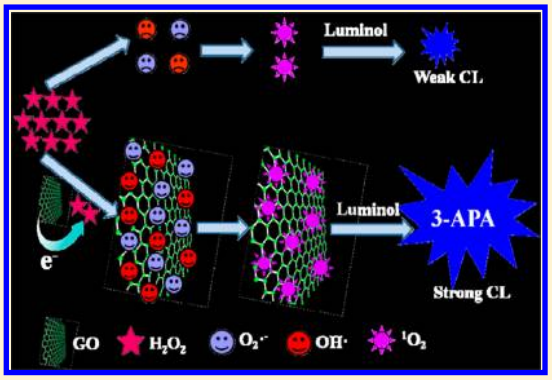

1. INTRODUCTION

Since the chemiluminescence (CL) phenomenon of luminol was first documented by Albrecht in 1928,[1] the luminol-H_2O_2 CL reaction has become most intensively studied and widely used, which can be catalyzed by various substances, including metal ions, metal complexes, peroxidases,[2−5] and so on. In recent years, the study of catalyzed luminol CL reactions was diverted from traditional molecular systems to nanoparticles (NPs)-enhanced systems for the purpose of higher sensitivity and stability, mainly taking advantage of the large surface area and special structure of nanomaterials.[6] In this case, the pioneer work initiated by Cui showed that the enhanced luminol CL was related to the sizes of AuNPs.[7] Similar phenomena have been reported since then, such as the use of PtNPs,[8] AgNPs,[9] gold/silver alloy NPs,[10] Co_3O_4 NPs,[11] ZnO NPs,[12] $CoFe_2O_4$ MNPs,[13] triangular AuNPs,[14] and so on. On the basis of their catalysis on luminol system, a great number of CL methods have been successfully developed and applied in various fields such as bioanalysis[15] and food analysis.[16] Because of the importance of luminol-H_2O_2 as a CL reaction, significant attention has been given to elucidate the chemiluminescent mechanism.

The CL of luminol has recently been reviewed by Barnett and Francis,[17] and the CL-producing processes of luminol involve a complex multistep pathway. Nowadays, it is generally accepted that oxygen- containing radicals, especially superoxide anion radical ($O_2^{\bullet-}$) and hydroxyl radical (OH•) as the important intermediates, have been involved in luminol oxidation processes.[18] The well-established mechanism[7,19,20] is that luminol can react with H_2O_2 to produce weak CL under alkaline conditions in the absence of any catalyst. The presence of traditional catalyst in the luminol-H_2O_2 system catalyzes the decomposition of H_2O_2, yielding some reactive intermediates such as OH• and $O_2^{\bullet-}$. The OH• then reacts with luminol to facilitate the generation of luminol radical ($L^{\bullet-}$), and further reaction between $L^{\bullet-}$ and $O_2^{\bullet-}$ produces the key intermediate hydroxy hydroperoxide, giving rise to the enhanced CL, as indicated in Scheme 1A. In fact, careful insight of relevant literatures showed that it was mainly OH• and $O_2^{\bullet-}$, rather than singlet oxygen ($^1O_2$), that directly led to the CL generation and enhancement of luminol, and there were very few reports about the CL induced by $^1O_2$ in aqueous media.[21] Although the photosensitized CL of luminol has been reported,[22] very low CL efficiency between luminol and $^1O_2$ was observed.[23]

Graphene, taking the form of single-atom-thick sheets of sp^2-bonded carbon atoms packed into a well-defined 2-D honeycomb structure, has attracted significant attention in a wide range of fields since its discovery in 2004.[24] As a novel

Received: June 20, 2012
Revised: September 16, 2012
Published: September 17, 2012

Scheme 1. Comparison of the CL Mechanism of Luminol Catalyzed by Traditional Catalyst (A) and GO (B)

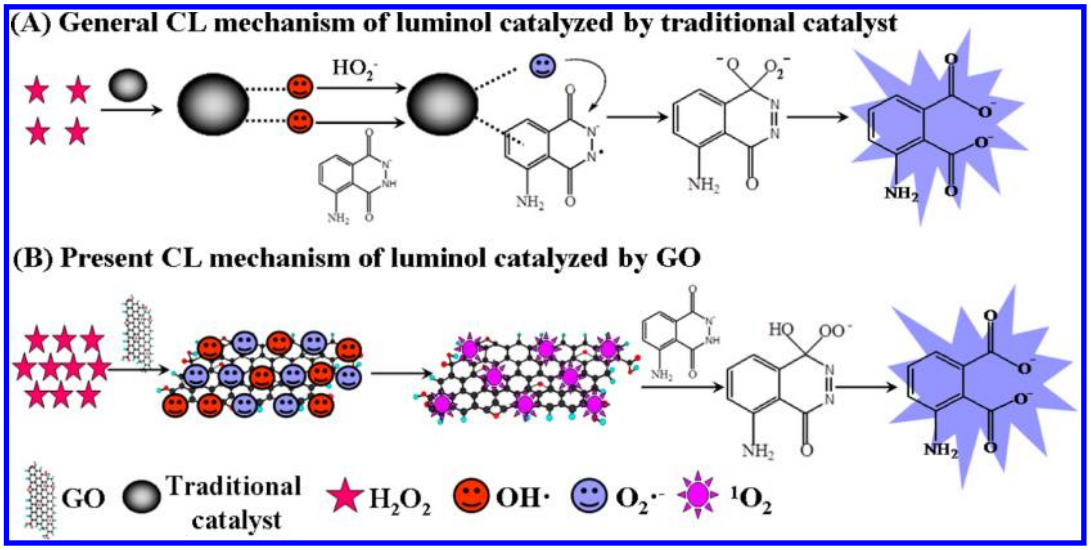

carbon nanomaterial, it has excellent thermal, optical, electronic, and mechanical properties. In particular, with extremely large specific surface area, good biocompatibility, and high adsorption capacity, graphene and its derivatives may have an intriguing potential for catalysis.[25−27] Up to date, the catalytic applications of carbon nanomaterials have focused primarily on the use of these materials either as supports for immobilizing catalytically active species or as metal-free catalysts.[28] Graphene oxide (GO), a chemically modified graphene sheet,[29,30] has multiple oxygen-related functional groups, such as hydroxyls and epoxides in the basal plane and carboxyl groups at the plane edges.[31] Therefore, with these oxygen-related groups, GO owned more active sites with unique catalytic activity compared with graphene.[26] For example, GO has been successfully used to make the oxidation of TMB by H_2O_2 to produce a blue color reaction on the basis of the intrinsic peroxidase property.[32] So far, investigations on the catalytic applications of GO in CL analysis are just in infancy, and no luminol CL system that directly employed GO as a catalyst has been reported, to the best of our knowledge.

In the present work, a surprising phenomenon was observed that a $^1O_2$-induced CL was greatly enhanced when GO was introduced into the luminol-H_2O_2 system. The $^1O_2$-induced CL enhancement became dominant due to the intrinsic catalysis of GO acting as the electron transfer accelerator and the $^1O_2$ generation proliferator. On the basis of this observation, a simple, rapid, and sensitive CL sensor for determinations of H_2O_2 and glucose was assembled.

2. EXPERIMENTAL SECTION

2.1. Chemicals and Solutions. A 0.01 M stock solution of luminol (3-aminophthalhydrazide) was prepared by dissolving 0.1772 g of luminol (Sigma, America) in 100 mL of 0.01 M NaOH solution and stored in a dark place for a few days before use. Working solutions of luminol were prepared by diluting the stock solution with 0.067 M Na_2HPO_4−KH_2PO_4 buffer solution. Working solutions of H_2O_2 were freshly prepared by appropriately diluting the commercial H_2O_2 (30% v/v) (Chuandong Chemical Engineering Reagent Factory, Chongqing, China), and their concentration was standardized by titration with $KMnO_4$.

Multiwalled carbon nanotubes (MWCNTs) were commercially purchased from Chengdu Organic Chemicals (Chinese Academy of Sciences, Chengdu, China), which were purified and oxidized according to the literature method.[33] Graphite powder was supplied by the Sinopharm Chemical Reagent (Shanghai, China). Carboxylic-acid-functionalized single-walled carbon nanotubes (SWCNTs) and glucose oxidase (GOD, 200 U/mg) were purchased from Sigma-Aldrich (St. Louis, MO). Other reagents for the synthesis of chemically converted graphene (CCG) and carbon nanoparticles (CNPs) such as hydrazine monohydrate, ammonia solution (28 wt % in water), and EDTA-2Na·$2H_2O$ were obtained from Chongqing Chemical Reagent Company (Chongqing, China). Glucose, fructose, lactose, and maltose were commercially available. Mili-Q purified water (18.2 MΩ) was used in all of these experimental processes.

The GO sheets were synthesized by a common Hummers method with slight modification.[34,35] The CCG and CNPs were prepared according to the method used in refs 36 and 37. The detailed information of the preparation of GO, CCG and CNPs is shown in the Supporting Information, and the characterization results of CCG and CNPs are presented in Figures S1 and S2 in the Supporting Information, respectively.

2.2. Apparatus. The CL spectra were drawn using a computerized BPCL ultraweak luminescence analyzer (Institute of Biophysics, Chinese Academy of Sciences, Beijing, China) with a series of high-energy optical filters of 230, 260, 290, 320, 350, 380, 400, 425, 440, 460, 490, 535, 555, 575, 620, and 640 nm between the CL flow cell and the PMT, as described in ref 38. The absorption spectra were measured with a UV-3600 UV−visible-NIR spectrophotometer (Shimadzu, Japan). The electron spin resonance (ESR) spectra were performed on a Bruker ESP-300 E spectrometer (Bruker, Germany). Transmission electron microscopy (TEM) measurement of GO was performed on a Tecnail 10 microscopy (Philips, Holland) at 100 kV. Fourier transform infrared (FT-IR) spectrophotometer (FTIR-8400S, Shimadzu, Japan) was used for recording the FT-IR spectra of GO, CCG, and CNPs.

2.3. General Procedure for CL Detection. The CL-producing reactions were carried out in a 3 mL quartz cuvette, and the signals were detected and recorded with the BPCL luminescence analyzer. In a typical experiment, 150 μL of H_2O_2

dx.doi.org/10.1021/jp306061u | J. Phys. Chem. C 2012, 116, 21622−21628

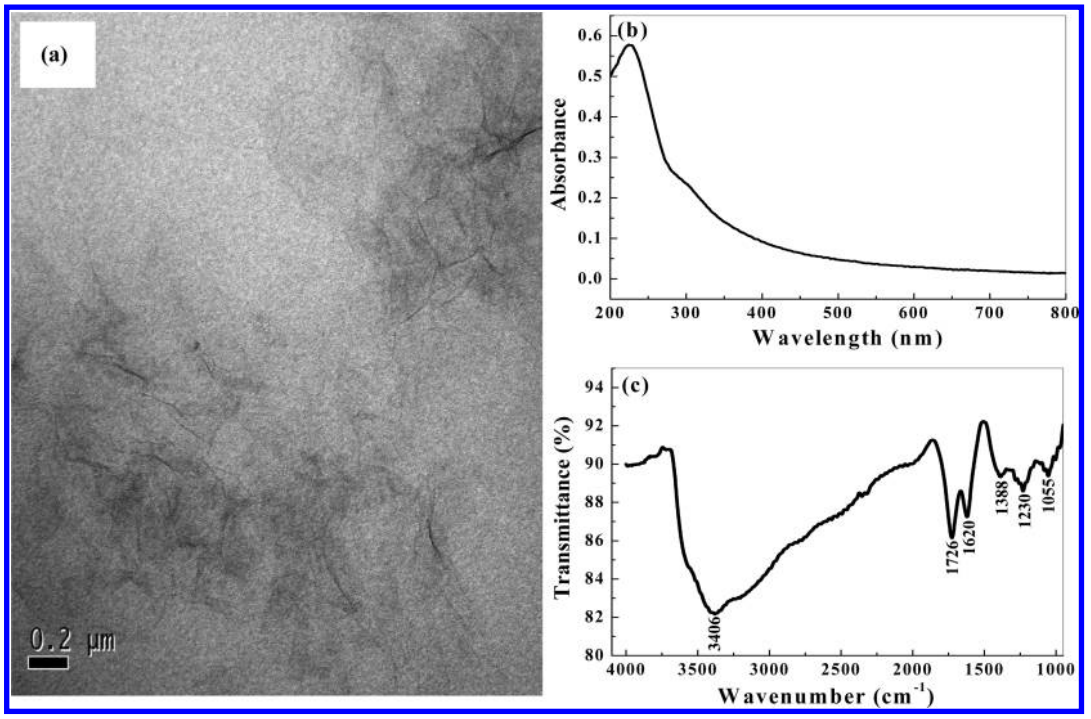

Figure 1. Features of the as-prepared GO. (a) TEM image, (b) UV−visible absorption spectrum, and (c) FT-IR spectrum of the as-prepared GO.

and 90 μL of aqueous solution of different carbon nanomaterials were added to the cuvette sequentially by an adjustable volume mechanical pipet; then, 250 μL of luminol solution was quickly injected by a microliter syringe. The CL profile and intensity were displayed and integrated for a 1 s interval at −1000 V.

As for investigating the effects of different radical scavengers on luminol-H_2O_2-GO system, the CL signals were monitored according to the same procedure as above, except 30 μL of radical scavengers with different concentrations was first mixed with H_2O_2 and GO solutions. The percentage of CL inhibition was calculated as $\Delta I/I_0 \times 100\%$, and the net CL intensity $\Delta I = I_0 - I$ showed the effects of radical scavengers on the CL of luminol-H_2O_2-GO system, where I_0 and I were the CL intensities without and with radical scavengers, respectively.

3. RESULTS AND DISCUSSION

3.1. Characterization of GO. The GO sheets were prepared using the Hummers method mentioned above, and their structure was successfully confirmed by the TEM analysis, UV−vis absorption spectroscopy, and FT-IR spectroscopy. After ultrasonic treatment for a few hours in water, GO is mostly single-layered or few-layered with clear wrinkles and folding on the surface and edge, as shown in Figure 1a. Figure 1b shows the typical UV−visible absorption spectrum of the as-prepared GO. It indicates that GO has a maximum absorption peak at 225 nm with a shoulder peak at ∼300 nm. Graphite powder was treated with H_2SO_4 and $KMnO_4$, and FT-IR studies could confirm the successful oxidation of graphite to GO. The FT-IR spectrum (Figure 1c) of the GO clearly shows an intense band at 3406 cm^{-1}, which was attributed to the OH groups, and band at 1726 cm^{-1}, which was typical of carbonyl groups. Besides, other C−O functionalities such as C−OH (1388 cm^{-1}), C−O−C (epoxy, 1230 cm^{-1}), and C−O (alkoxy, 1055 cm^{-1}) are also clearly visible. In addition, the peak at 1620 cm^{-1} could be assigned to the skeletal vibrations of unoxidized graphitic domains and the vibrations of the adsorbed water molecules.[39] The introduction of oxygenated functional groups on carbon sheets not only enhanced the hydrophilicity but also provided an insight into the excellent catalytic activity of GO.

3.2. Enhanced CL of Luminol. The effects of different carbon nanomaterials on the CL of luminol-H_2O_2 system were investigated. As Figure 2 shows, the CL between luminol and

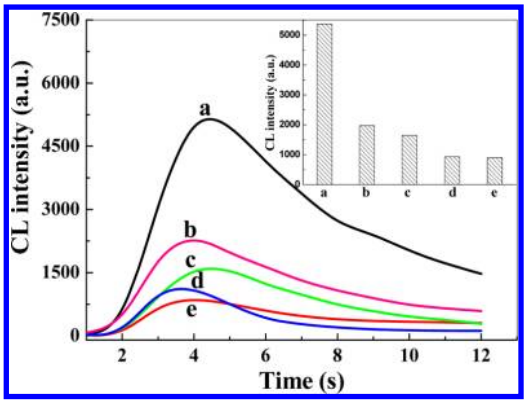

Figure 2. Kinetic monitoring on luminol-H_2O_2 CL in the presence of (a) GO, (b) CNPs, (c) MWCNTs, (d) SWCNTs, and (e) H_2O. The inset shows the initial maximum CL intensities of the above five different systems. Final concentrations: luminol, 2.0×10^{-4} M in 0.067 M Na_2HPO_4−KH_2PO_4 buffer solution (pH 8.67); H_2O_2, 30 μM; GO, CNPs, MWCNTs, or SWCNTs, 45 μg/mL.

H_2O_2 is a relatively slow reaction process, and very weak CL can be obtained. In the presence of varieties of carbon nanomaterials including GO, CNPs, MWCNTs, or SWCNTs, however, the CL of luminol-H_2O_2 system gets enhanced. With the same concentration (45 μg/mL) of the above carbon nanomaterials, the GO-enhanced CL is markedly stronger than that of the other carbon materials, reaching the maximum value rapidly. The enhanced CL signals were possibly ascribed to the

dx.doi.org/10.1021/jp306061u | J. Phys. Chem. C 2012, 116, 21622−21628

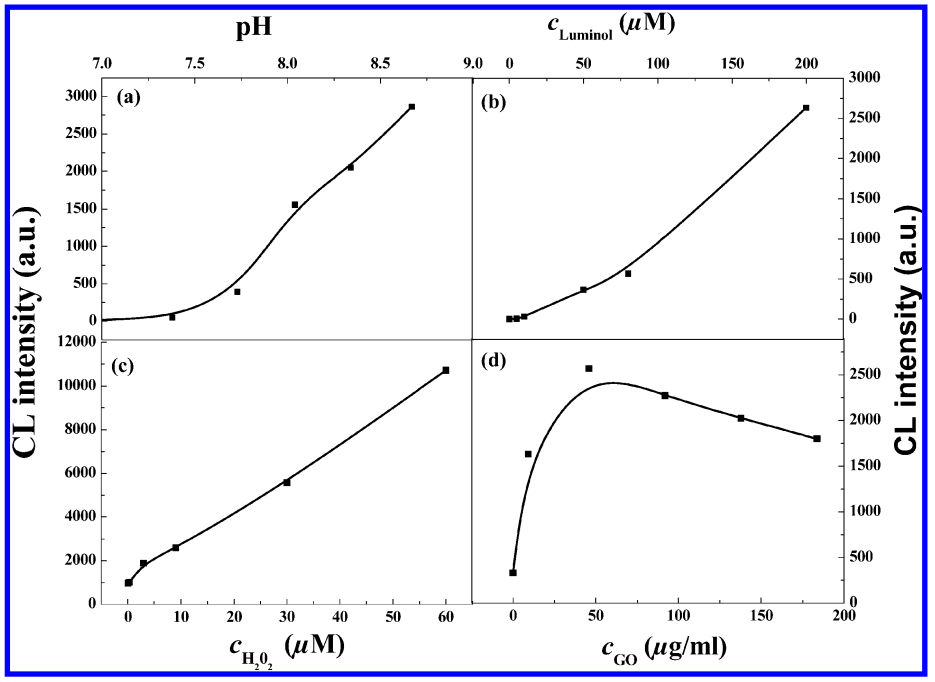

Figure 3. Effects of the reactant conditions on luminol-H_2O_2-GO CL system. (a) Effects of luminol pH: 2.0×10^{-4} M luminol, 9.0 μM H_2O_2, 45 μg/mL GO. (b) Effects of luminol concentration: 0.067 M Na_2HPO_4–KH_2PO_4 buffer solution (pH 8.67), 9.0 μM H_2O_2, 45 μg/mL GO. (c) Effects of H_2O_2 concentration: 2.0×10^{-4} M luminol in 0.067 M Na_2HPO_4–KH_2PO_4 buffer solution, 45 μg/mL GO. (d) Effects of GO concentration: 2.0×10^{-4} M luminol in 0.067 M Na_2HPO_4–KH_2PO_4 buffer solution, 9.0 μM H_2O_2.

catalysis from carbon nanomaterials. It has been demonstrated that the rate of heterogeneous catalysis is increased with increasing the available active surface area of the catalyst.[40,41] Accordingly, the higher surface area of GO (calculated value, 2630 m^2/g,[42] larger than MWCNTs and SWCNTs[43,44]) plays a critical role in the catalytic activity during the luminol CL processes. Moreover, GO presents high affinity to organic substrates via $\pi-\pi$ and hydrophobic interactions because of its unique structure. Therefore, in our opinion, luminol can be adsorbed on the surface of graphene and donate lone-pair electrons of the amino groups to graphene. This can lead to an increase in electron density of graphene, and higher electron density would be advantageous for CL.[7]

If luminol was injected into the mixture of H_2O_2 and CCG, however, different phenomena were observed, and the effect of CCG on luminol CL seemed to be much weaker than that of GO (Figure S3, Supporting Information). As we know, CCG is derived from GO by chemical reduction, which can eliminate the majority of the oxygen functional groups and restore the conjugated structure from GO.[45] Therefore, this indicates that these oxygen-related groups are indeed a reactive part in the present system and should be crucial for luminol CL. In other words, oxygen functional groups-rich materials, such as GO, show high catalytic activity under certain conditions. In conclusion, GO presents the strongest catalysis compared with other carbon nanomaterials, which is mainly because of the high active surface area, multiple surface oxygen-related functional groups and unique electronic structure. Therefore, the luminol-H_2O_2-GO system was chosen as a model for further studies, and the optimized conditions (Figure 3) were as follows.

This CL took place in Na_2HPO_4–KH_2PO_4 buffer solution (pH 8.67) and was greatly different from the commonly reported luminol CL, which was more favored under the strongly basic medium such as NaOH solution. The optimized concentrations of luminol and GO are 2×10^{-4} M and 45 μg/mL. Besides, the CL of the above system also depends on the concentration of H_2O_2; different concentration of H_2O_2 is selected according to the signal intensity in the subsequent experiments.

3.3. Spectral Features of Luminol CL Catalyzed by GO.

The CL spectra were measured using high-energy cutoff filters of various wavelengths. Figure 4 displays that luminol-H_2O_2 CL

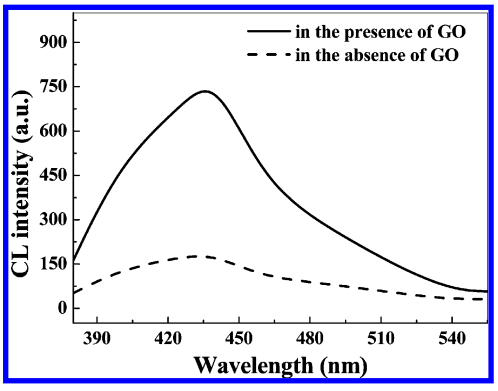

Figure 4. Chemiluminescent spectra of luminol-H_2O_2 system in the presence or absence of GO. Final concentrations: luminol, 2.0×10^{-4} M in Na_2HPO_4–KH_2PO_4 buffer solution (pH 8.67); H_2O_2, 30 μM; GO, 45 μg/mL.

in either the presence or the absence of GO has the maximum emission at 440 nm, revealing that the luminophors in both cases are the same species, namely, the excited-state 3-aminophthalate anions (3-APA*). Therefore, the addition of GO did not lead to the generation of a new emitter for this CL system, and GO acted only as a reagent to enhance the CL signals, which are the same as those described nanocatalysis on the luminol-H_2O_2 system previously.[8−13]

dx.doi.org/10.1021/jp306061u | J. Phys. Chem. C 2012, 116, 21622−21628

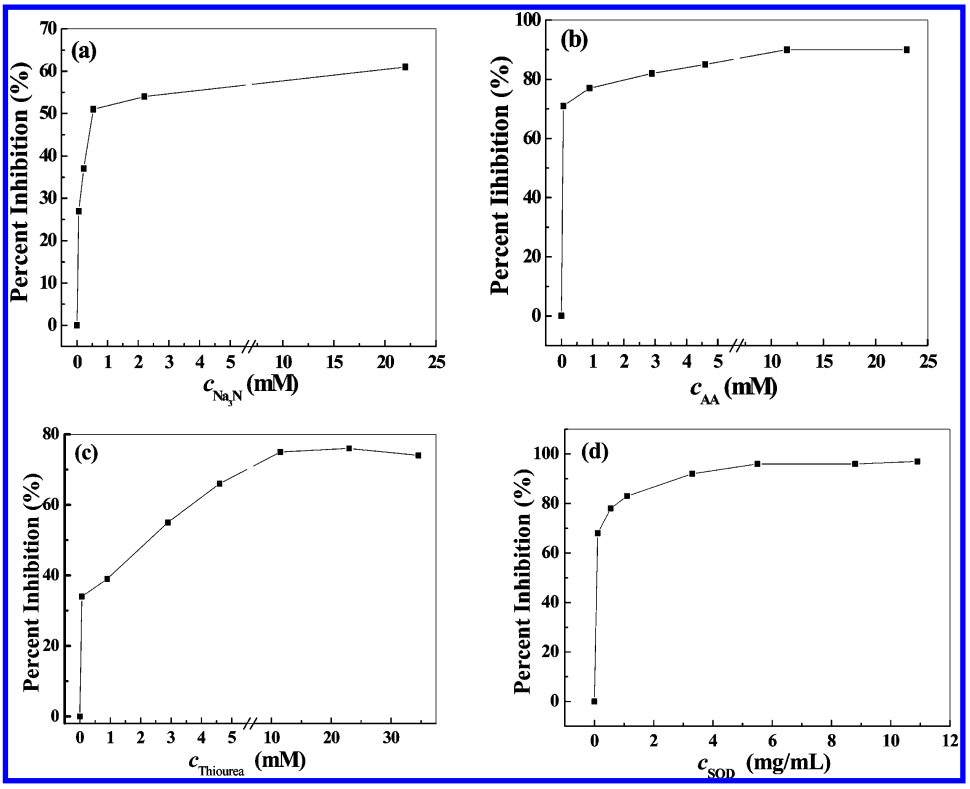

Figure 5. Effects of the radical scavengers of (a) Na_3N, (b) AA, (c) thiourea, and (d) SOD on the luminol-H_2O_2-GO CL system. Final concentrations: luminol, 2.0×10^{-4} M in Na_2HPO_4–KH_2PO_4 buffer solution (pH 8.67); H_2O_2, 9.0 μM; GO, 45 μg/mL.

As stated above, the reaction between luminol and H_2O_2 generates weak CL, and GO may be involved in this CL reaction as an efficient catalyst. In this case, GO should still remain unchanged after the reaction to confirm that UV–visible absorption experiments were carried out to characterize the GO before and after the CL reaction (Figure S4, Supporting Information). In fact, GO has a maximum absorption band characterized at 225 nm, whereas the luminol-H_2O_2 system has two absorption bands characterized at 297 and 348 nm, respectively. As can be seen, the absorbance of the luminol-H_2O_2-GO system is nearly equal to the sum of the absorbance of the above two individual systems, on the one hand, and there is no significant difference in the position of the maximum absorption between the as-prepared GO and that after the CL experiments, on the other hand. This demonstrated that there was no new species formed in the presence of GO, further proving that the CL enhancement of luminol-H_2O_2 system should be ascribed to the catalytic effect of GO.

3.4. Observation of the $^1O_2$-Induced Luminol CL. An unusual $^1O_2$-induced CL was observed in the above CL system, which could be identified by using specific quencher for $^1O_2$ such as sodium azide (NaN_3).[46] As Figure 5a shows, the addition of NaN_3 can effectively inhibit the CL, and the inhibited percentage gets increased with increasing the concentration of NaN_3. For instance, ~61% CL intensity was inhibited by the high concentration (22.0 mM) of NaN_3. The other $^1O_2$ scavenger was also available, and the addition of 50.0 mM dimethylfuran could quench 65% of the original CL intensity. On the basis of these experimental data, the generation of $^1O_2$ in the luminol-H_2O_2-GO system was identified, suggesting a potential $^1O_2$-dependent CL mechanism.

To elucidate further the generation and contribution to the observed CL of $^1O_2$, we explored room-temperature ESR spectroscopy. 5,5-Dimethyl-1-pyrroline N-oxide (DMPO), a specific target molecule of OH·,[47] was used for exploring the existence of OH· during the luminol oxidation processes. The ESR spectrum (Figure 6a) presents a characteristic peak of the typical DMPO–OH· adduct in luminol-H_2O_2 system, whereas no such signal is observed when DMPO was introduced into the luminol-H_2O_2-GO system. This phenomenon proved that OH· was formed and reacted with $O_2^{\cdot-}$ to produce $^1O_2$ in the presence of GO because the $O_2^{\cdot-}$ was more stable in high pH solution, and GO could improve the radical species stability as well.[48] 2,2,6,6-Tetramethyl-4-piperidine (TEMP) is a specific target molecule of $^1O_2$ because the reaction of $^1O_2$ with TEMP results in the formation of the adduct 2,2,6,6-tetramethyl-4-piperidine-*N*-oxide (TEMPO),[49] which is a stable nitroxide radical with a characteristic spectrum. Figure 6b (black line) shows the strongly specific signals of TEMPO, which supports the generation of $^1O_2$ in the luminol-H_2O_2 system. However, the characteristic signal intensity of TEMPO decreases more than 50% (red line, Figure 6b) when TEMP was added to the mixture solution of GO, luminol, and H_2O_2. These novel observations revealed that the abundant $^1O_2$ was consumed quickly in this solution because the addition of GO could not only accelerate the decomposition of H_2O_2 but also facilitate greatly the CL reaction between $^1O_2$ and luminol, thus leading to a great increase in CL intensity. That is, the CL in the luminol-H_2O_2-GO system was primarily caused by $^1O_2$ rather than other oxygen-centered radicals (e.g., $O_2^{\cdot-}$).

3.5. Possible Mechanism of the Enhanced CL Reaction. The CL systems of metal-ions-catalyzed luminol-H_2O_2 have been extensively investigated, and the catalysis is attributed to the fact that they can accelerate the breakdown of

dx.doi.org/10.1021/jp306061u | J. Phys. Chem. C 2012, 116, 21622–21628

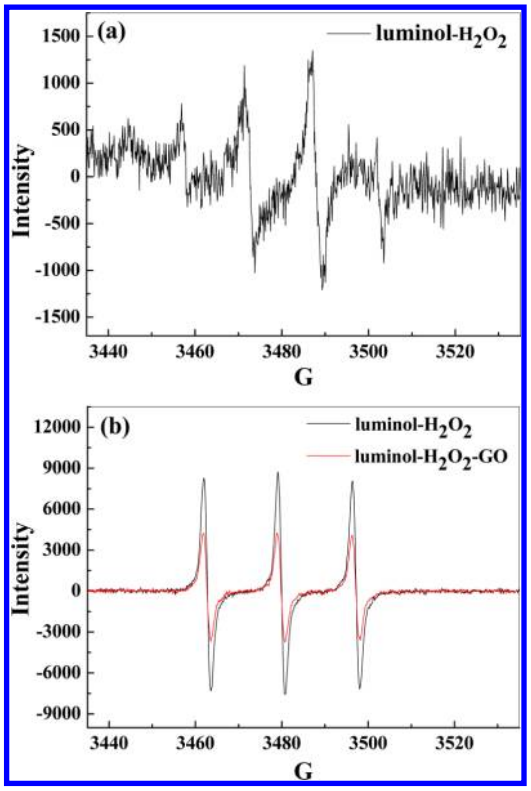

Figure 6. (a) ESR spectrum of DMPO−OH• adduct in luminol-H_2O_2 system and (b) ESR spectra of nitroxide radicals generated by reaction of TEMP probe in the luminol-H_2O_2 system and the luminol-H_2O_2-GO system. Conditions: receiver gain, 1.00e + 05; modulation amplitude, 1 G; sweep width, 100.00 G; microwave power, 1.00e + 01 mW. The ESR measurements were achieved with a Bruker ESP-300E spectrometer operating in the X-band at room temperature.

H_2O_2 to generate some strong oxidizing species, which is indispensable for luminol CL.[2,3] In the luminol-H_2O_2-GO system, besides the important observation of the $^1O_2$-induced CL, other oxidizing radical species may also occur. As for GO, when it was added to alkaline H_2O_2 solution, violent reaction took place as many bubbles occurred. So in this case, it is assumed that the rich electrons of GO might transfer to H_2O_2,[32] and this can cause the decomposition of H_2O_2 efficiently, yielding much more radical intermediates due to the acceleration of the radical species generation by GO.[48]

The formation of these intermediates could be identified by quenching CL experiments with the addition of the radical scavengers. Ascorbic acid (AA) is a common free radical scavenger, and a sharp decrease in CL signals can be observed even if very low concentration of AA is introduced into the above system. For instance, the CL decreases ~90.0% with the addition of 11.5 mM AA (Figure 5b), which confirms the radical reaction mechanism in the GO-catalyzed luminol-H_2O_2 system. OH• was considered to be one of the most potent oxidizers among the oxygen-related radicals and could be effectively scavenged by thiourea.[50] Figure 5c shows the CL percentage inhibition increases with increasing the concentration of thiourea. As an assistant detection method, it indicates that OH• is produced in the mixing solutions and might greatly contribute to the CL, in agreement with the above result by ESR spectroscopy. Superoxide dismutase (SOD) was frequently used for the detection of $O_2^{\bullet-}$.[51] In the above examined CL systems, the generation of $O_2^{\bullet-}$ was confirmed with the significantly quenching effects upon the addition of SOD. SOD nearly completely inhibits the light emission at a concentration of 10.9 mg/mL, as displayed in Figure 5d.

In view of the above results, it could be concluded that these radical intermediates generated during the decomposition of H_2O_2 were the key species for producing $^1O_2$. That is, $^1O_2$ was a product of an interaction between these reactive oxygen species, which was corresponding to a previously suggested generation mechanism of $^1O_2$ in the presence of metal ions and H_2O_2.[52] Therefore, the enhancing effect of GO on the luminol-H_2O_2 system should be attributed to the $^1O_2$-induced CL mechanism, revealing a different route from the universally accepted catalysis mechanism, as summarized in Scheme 1B.

When GO was added to the luminol-H_2O_2 system, an electron-transfer process between GO and H_2O_2 occurred, and this could catalyze the decomposition of H_2O_2 to yield much more active radical species, such as OH• and $O_2^{\bullet-}$. The recombination reaction of OH• and $O_2^{\bullet-}$ would take place to form a high yield of $^1O_2$ on the surface of GO, then the produced $^1O_2$ reacted with luminol anion, generating an unstable endoperoxide. The endoperoxide decomposed to the 3-APA*, which returned to the ground-state accompanied by an enhanced emission.[53] However, the experiments above only demonstrated that a major fraction of the CL was induced by $^1O_2$, and a small fraction of CL possibly caused by $O_2^{\bullet-}$ could not be totally ruled out.

3.6. Detection of H_2O_2 and Glucose. Because the GO-enhanced luminol CL was dependent on the concentration of H_2O_2, it could be applied directly to detect H_2O_2. Under the optimized conditions described above, the CL was proportional to the concentration of H_2O_2 in the range of 0.09−60 μM with the detection limit of 0.03 μM (3σ). When the above CL reaction was coupled to the glucose catalytic reaction by GOD, the proposed CL method could be easily achieved to detect glucose. It was performed in two separated steps: (1) the catalytic oxidation of glucose in the presence of GOD was carried out in PBS (10 mM, pH 7.4) at 37 °C for 30 min and (2) the amount of H_2O_2 produced in the first step was further determined using the luminol-H_2O_2-GO system. The results showed that this method had a good linear range of 1.6−600 μM, with the detection limit as low as 0.78 μM (3σ) for the detection of glucose. Moreover, several control experiments using fructose, lactose, and maltose were taken to investigate the selectivity of the proposed method. The CL signals of these glucose analogues remained nearly the same as the background signal (except for a little response for maltose), with their concentrations as high as 5 mM (Figure S5, Supporting Information). This indicated that the CL system developed here showed good specificity toward glucose detection.

4. CONCLUSIONS

In summary, we have demonstrated that GO could catalyze the CL of luminol-H_2O_2 system in a weakly basic medium. Because of the high active surface area, multiple surface oxygen-containing functional groups, and unique electronic structure, GO presented the strongest catalysis toward luminol CL than that of other carbon nanomaterials such as CNPs, MWCNTs, SWCNTs, and CCG. The CL of the luminol-H_2O_2-GO system was also the emission from the 3-APA*, indicating that GO served as a catalyst onlyto accelerate electron-transfer processes and the $^1O_2$ generation on its surface. Therefore, the CL should occur through the intermediate of $^1O_2$, rather than other

dx.doi.org/10.1021/jp306061u | J. Phys. Chem. C 2012, 116, 21622−21628

intermediates such as $O_2^{\bullet-}$ in the presence of the traditional catalyst that occurred in a strongly basic medium. Moreover, the present GO-based CL assay depended on the use of pH 8.67 Na_2HPO_4–KH_2PO_4 buffer solution as a reaction medium, which may improve the selectivity and biocompatibility of luminol system to some extent. This work not only displays a new application of GO in CL field and enriches luminol CL mechanism but also will be of great potential applications in analytical and biochemical fields. Further research into the applications of the proposed CL system is in progress.

■ ASSOCIATED CONTENT

Supporting Information

Preparation of GO, CCG, and CNPs; characterization of CCG and CNPs; UV–visible absorption spectra of luminol, GO, luminol-H_2O_2 system, and luminol-H_2O_2-GO system, respectively; and specificity for glucose detection with the proposed CL method. This material is available free of charge via the Internet at http://pubs.acs.org.

■ AUTHOR INFORMATION

Corresponding Author

*E-mail: chengzhi@swu.edu.cn; Fax: (+86) 23 68866796; Tel: (+86) 23 68254659.

Notes

The authors declare no competing financial interest.

■ ACKNOWLEDGMENTS

We are grateful to the financial supports from the National Natural Science Foundation of China (NSFC, 21035005) and the Natural Science Foundation Project of China SWU (SWU208015).

■ REFERENCES

(1) Albrecht, H. O. *Z. Phys. Chem.* **1928**, *136*, 321.
(2) Lin, J.-M.; Shan, X.; Hanaoka, S.; Yamada, M. *Anal. Chem.* **2001**, *73*, 5043.
(3) Burdo, T. G.; Seltz, W. R. *Anal. Chem.* **1975**, *47*, 1639.
(4) Bostick, D. T.; Hercules, D. M. *Anal. Chem.* **1975**, *47*, 447.
(5) Schneider, E. *J. Am. Chem. Soc.* **1941**, *63*, 1477.
(6) Giokas, D. L.; Vlessidis, A. G.; Tsogas, G. Z.; Evmiridis, N. P. *TrAC, Trends Anal. Chem.* **2010**, *29*, 1113.
(7) Zhang, Z.-F.; Cui, H.; Lai, C.-Z.; Liu, L.-J. *Anal. Chem.* **2005**, *77*, 3324.
(8) Xu, S.-L.; Cui, H. *Luminescence* **2007**, *22*, 77.
(9) Chen, H.; Gao, F.; He, R.; Cui, D. *J. Colloid Interface Sci.* **2007**, *315*, 158.
(10) Li, S.; Tao, S.; Wang, F.; Hong, J.; Wei, X. *Microchim. Acta* **2010**, *169*, 73.
(11) Xie, J.; Huang, Y. *Anal. Methods* **2011**, *3*, 1149.
(12) Li, S.-F.; Zhang, X.-M.; Du, W.-X.; Ni, Y.-H.; Wei, X.-W. *J. Phys. Chem. C* **2009**, *113*, 1046.
(13) He, S.; Shi, W.; Zhang, X.; Li, J.; Huang, Y. *Talanta* **2010**, *82*, 377.
(14) Li, Q.; Liu, F.; Lu, C.; Lin, J.-M. *J. Phys. Chem. C* **2011**, *115*, 10964.
(15) Li, Q.; Zhang, L.; Li, J.; Lu, C. *TrAC, Trends Anal. Chem.* **2011**, *30*, 401.
(16) Liu, M.; Lin, Z.; Lin, J.-M. *Anal. Chim. Acta* **2010**, *670*, 1.
(17) Barnett, N. W.; Francis, P. S. *Chemiluminescence: Liquid-Phase, Encyclopedia of Analytical Science*, 2nd ed.; Elsevier Academic Press: London, 2005.
(18) Merenyi, G.; Lind, J. S. *J. Am. Chem. Soc.* **1980**, *102*, 5830.
(19) Merényi, G.; Lind, J.; Eriksen, T. E. *J. Biolumin. Chemilumin.* **1990**, *5*, 53.
(20) Yuan, D.-Q.; Lu, J.; Atsumi, M.; Yan, J.-M.; Kai, M.; Fujita, K. *Org. Biomol. Chem.* **2007**, *5*, 2932.
(21) Lu, J.; Lau, C.; Morizono, M.; Ohta, K.; Kai, M. *Anal. Chem.* **2001**, *73*, 5979.
(22) Kuschnir, K.; Kuwana, T. *J. Chem. Soc. D* **1969**, 193.
(23) Yasuta, N.; Takahashi, S.; Takenaka, N.; Takemura, T. *Bull. Chem. Soc. Jpn.* **1999**, *72*, 1997.
(24) Novoselov, K. S.; Geim, A. K.; Morozov, S. V.; Jiang, D.; Zhang, Y.; Dubonos, S. V.; Grigorieva, I. V.; Firsov, A. A. *Science* **2004**, *306*, 666.
(25) Xiang, Q.; Yu, J.; Jaroniec, M. *Chem. Soc. Rev.* **2012**, *41*, 782.
(26) Machado, B. F.; Serp, P. *Catal. Sci. Technol.* **2012**, *2*, 54.
(27) Pyun, J. *Angew. Chem., Int. Ed.* **2011**, *50*, 46.
(28) Serp, P.; Figueiredo, J. L. *Carbon Materials for Catalysis*, John Wiley & Sons: Hoboken, NJ, 2009.
(29) Cote, L. J.; Kim, F.; Huang, J. *J. Am. Chem. Soc.* **2009**, *131*, 1043.
(30) Dikin, D. A.; Stankovich, S.; Zimney, E. J.; Piner, R. D.; Dommett, G. H. B.; Evmenenko, G.; Nguyen, S. T.; Ruoff, R. S. *Nature* **2007**, *448*, 457.
(31) Park, S.; Ruoff, R. S. *Nat. Nanotechnol.* **2009**, *4*, 217.
(32) Song, Y.; Qu, K.; Zhao, C.; Ren, J.; Qu, X. *Adv. Mater.* **2010**, *22*, 1.
(33) He, P.; Bayachou, M. *Langmuir* **2005**, *21*, 6086.
(34) Hummers, W. S.; Offeman, R. E. *J. Am. Chem. Soc.* **1958**, *80*, 1339.
(35) Xu, Y.; Bai, H.; Lu, G.; Li, C.; Shi, G. *J. Am. Chem. Soc.* **2008**, *130*, 5856.
(36) Li, D.; Müller, M. B.; Gilje, S.; Kaner, R. B.; Wallace, G. G. *Nat. Nanotechnol.* **2008**, *3*, 101.
(37) Pan, D.; Zhang, J.; Li, Z.; Wu, C.; Yan, X.; Wu, M. *Chem. Commun.* **2010**, *46*, 3681.
(38) Lin, J.-M.; Liu., M. *J. Phys. Chem. B* **2008**, *112*, 7850.
(39) Xu, Y.; Bai, H.; Lu, G.; Li, C.; Shi, G. *J. Am. Chem. Soc.* **2008**, *130*, 5856.
(40) Sharma, R. K.; Sharma, P.; Maitra, A. *J. Colloid Interface Sci.* **2003**, *265*, 134.
(41) Henglein, A. *J. Phys. Chem.* **1993**, *97*, 5457.
(42) Peigney, A.; Laurent, Ch.; Flahaut, E.; Bacsa, R. R.; Rousset, A. *Carbon* **2001**, *39*, 507.
(43) Wang, F.; Zhang, K. *J. Mol. Catal. A: Chem.* **2011**, *345*, 101.
(44) Ajayan, P. M. *Chem. Rev.* **1999**, *99*, 1787.
(45) Xu, Y.; Zhao, L.; Bai, H.; Hong, W.; Li, C.; Shi, G. *J. Am. Chem. Soc.* **2009**, *131*, 13490.
(46) Harbour, J. R.; Issler, S. L. *J. Am. Chem. Soc.* **1982**, *104*, 903.
(47) Villamena, F. A.; Locigno, E. J.; Rockenbauer, A.; Hadad, C. M.; Zweier, J. L. *J. Phys. Chem. A* **2007**, *111*, 384.
(48) Wang, Y.; Lu, J.; Tang, L.; Chang, H.; Li, J. *Anal. Chem.* **2009**, *81*, 9710.
(49) Li, H.-R.; Wu, L.-Z.; Tung, C.-H. *J. Am. Chem. Soc.* **2000**, *122*, 2446.
(50) Wang, W.-F.; Schuchmann, M. N.; Schuchmann, H.-P.; Knolle, W.; Sonntag, J. V.; Sonntag, C. V. *J. Am. Chem. Soc.* **1999**, *121*, 238.
(51) Schaap, A. P.; Thayer, A. L.; Faler, G. R.; Goda, K.; Kimura, T. *J. Am. Chem. Soc.* **1974**, *96*, 4025.
(52) Aboul-Enein, H. Y.; Kruk, I.; Lichszteld, K. *Biospectroscopy* **1998**, *4*, 229.
(53) Foote, C. S. *Photochem. Photobiol.* **1991**, *54*, 659.